Supporting Information

Optical characterization of a two-dimensional BODIPY-based polymer material and its related chromophores

P. Piatkowski[1,2], M. Moreno[3], M. Liras[4,5], F. Sánchez[5] and A. Douhal[1*]

[1] Departamento de Química Física, Facultad de Ciencias Ambientales y Bioquímica, and Inamol, Universidad de Castilla-La Mancha, Avenida Carlos III, S.N., Toledo 45071, Spain

[2] Department of Chemistry, University of Warsaw, Żwirki i Wigury 101, 02-089 Warsaw, Poland

[3]Departament de Química, Universitat Autónoma de Barcelona, Bellaterra, 08193 Barcelona, Spain

[4] IMDEA-Energía Parque Tecnológico de Móstoles Avda. Ramón de la Sagra, 3, 28935 Móstoles, Madrid, Spain

[5]Instituto de Química Orgánica General IQOG-CSIC Juan de la Cierva, 3 28006 Madrid Spain

* Corresponding author: Abderrazzak.Douhal@uclm.es

Theoretical calculations

MD1. Optimization of the molecule in the ground electronic state reveals that the system is almost planar and only two fluorine atoms and hydrogens of the methyl groups are found symmetrically out the plane that contains the rest of the atoms. Therefore it belongs to the C_{2v} group of symmetry. Scheme S1 depicts the obtained geometry. The full set of Cartesian Coordinates is given in the SI section.

A TDDFT calculation at the equilibrium geometry gives the energies of the lowest singlet excited electronic states. The oscillator strengths between the ground and the excited electronic states are also obtained. As those results give a direct measure of the absorption intensity, a theoretical absorption spectrum of MD1 can be obtain (Scheme S1).

Three active bands are predicted from the calculations (bands above 200 nm have not been calculated as this high energy range has not been experimentally explored). The most intensive one (571 nm, oscillator strength (f) 1.14) corresponds to the HOMO→LUMO transition. The second, less intense band (f = 0.65), is predicted to peak at 405 nm. This excitation mainly arises from the HOMO–2→LUMO transition. Finally a third absorption band, almost as intense as the first one (f = 0.93), is found at 322 nm. The main contribution to this excitation comes from the HOMO→LUMO+1 transition. It has to be noted that the transition to the second excited electronic state (S_2) peaking at 462 nm has small oscillator strength of 0.05 (Figure S2). The other two active bands correspond to the excitation to the third (S_3) and fourth (S_4) excited states respectively. At shorter wavelengths (higher energies) other states with small transition probabilities are found. Among these S_{10} at 304 nm is the only one with a non-negligible oscillator strength (f = 0.11). As seen in Figure S2 all these states are not making any relevant contribution to the shape of the absorption spectrum. It is accepted that electronic states

with oscillator strength below 0.1 are “dark” states (i.e: states that cannot be accessed by light irradiation of the ground electronic state).

The molecular orbitals implied in the allowed excitations are depicted in Figure S3. It is clear that all orbitals are of π type. Obviously the most interesting transition is the S_0 to S_1 as this one will mainly govern the photochemistry of MD1. Analysis of the HOMO and LUMO states, the orbitals mainly implied in the S_1 excitation, points to a noticeable degree of internal charge transfer from the two lateral phenylacetylene rings to the BODIPY central part of the molecule. Analysis of the Mulliken charges allows quantifying this transfer: the total charge in the two phenylacetylene groups increases by 0.2378 u.a. upon S_0 to S_1 electronic excitation. The ulterior nuclear relaxation in S_1 slightly increases this internal charge transfer up to 0.2750 a.u.

The optimized geometry in the S_1 state does not noticeably differ from the one in the ground state depicted in Figure S3. It maintains the C_{2v} symmetry and only minor differences in the bond distances are to be noted. The observed differences confirm the change in bonding/antibonding character between the HOMO and LUMO for adjacent atoms. The Cartesian Coordinates of this structure are given in the SI section. The final energy of the structure gives a theoretical estimate of the main emission band of MD1 that is predicted to peak at 625 nm. The HOMO and LUMO, again the orbitals mainly implied in the de-activation from S_1 to S_0, are also very similar to the ones depicted in Figure S3.

Finally we have studied the rotation of the terminal phenyl groups in order to see whether the two (equivalent) structures resulting from the rotation are freely interconverting at room temperature. A reaction coordinate calculation reveals that the maximum of energy along the phenyl rotation is at 90º (hardly a surprising fact) and that the energy barrier for this rotation is very small, 1.00 kcal/mol, so that free rotation is

predicted at least in gas phase. The viscosity of the solvent, not considered in our theoretical calculations could seriously hinder such a rotation.

MD2. Large MD2 molecular structure is a very symmetric one. Our calculations at the ground electronic state confirm that this molecule belongs to the D_{3h} symmetry group (the three "branches" out of the central phenyl ring are equivalent). Scheme S2 depicts the theoretically calculated equilibrium geometry. The full Cartesian Coordinates are to be found in the SI section.

At the equilibrium geometry in S_0 the calculation of the lowest energy excited electronic state reveals quite complicated pattern of excitations as some excited states are now degenerate (as expected from the D_{3h} symmetry group). In any case the absorption spectra can be predicted from these results and the final shape is depicted in Figure S5.

Again, the transition to the first singlet excited electronic state S_1 has the highest probability. It peaks at 521 nm and has quite large oscillator strength of 1.38. Our results also disclose that the S_1 state is double degenerated. Disregarding the dark states, the next allowed transition (f = 0.15) is found at 470 nm and it is also doubly degenerate. The excited states accessed from this excitation are S_7 and S_8. The transitions form S_0 to S_3 and to S_6 can be considered as dark states due to low oscillator strengths (less than 0.1). Next bright states are two fully degenerate S_{10} and S_{11} states with f = 0.48 (401 nm). The third almost degenerate state S_{12} also peaks at 401 nm but it has a smaller (f = 0.27) transition probability. The next allowed transition is found at 372 nm. It corresponds to a transition to a double degenerate state (S_{16} and S_{17}) with modest activity (f = 0.22). The last bright state in the relevant zone of the electromagnetic spectrum is found at 338 nm. It is attributed to transitions from S_0 to S_{23} and S_{24} (doubly degenerate) and it is one of the most intensive bands (f=0.61). The energies of those last states are more prone to large

numerical errors as the theoretical calculation has included just 25 excited states. All other states are dark states in the above described sense.

The analysis of the molecular orbitals implied in the electronic excitation is now a quite complicated task. The largely extended π system of the molecule provokes that the energy differences between adjacent orbitals are small and so the excitation pattern that leads to a given excited state cannot be restricted to just one excitation (as done for MD2 above). Additional complications in MD2 come from the high symmetry of the molecule as now some orbitals are degenerate (this is the case of both the HOMO and the LUMO). For instance, the most probable transition from S_0 to S_1 (and the degenerate S_2) has 14 excitations with coefficients higher than 0.1. A qualitative analysis of the molecular orbitals involved in the transition in order to grasp the electronic rearrangement upon excitation is therefore unattainable. Alternatively we will look at the charges in all the atoms of the molecule in order to see relevant changes in the charge distributions upon electronic excitation.

The optimization of MD2 in the S_1 state does not apparently produce large variations in the molecular geometry. However there are slight modifications of bond distances that eventually break the whole symmetry of the molecule that only retains the molecular plane of symmetry (C_S). The most noticeable effect of the lowering in the symmetry is that the molecular orbitals are no longer degenerate. Although, as the deviations from the symmetric positions are tiny, there are very small energy differences between the degenerate pairs of the excited states. This makes the analysis of the emission spectrum, depicted in Figure S8, more complex. The lowest energy (highest wavelength) transition to S_1 is predicted to peak at 586 nm. It mainly involves the HOMO→LUMO transition and is clearly allowed (f = 0.80), though it has not the highest probability as the $S_0 \rightarrow S_2$ transition, peaking at 529 nm has an oscillator strength of f = 0.91. S_2 comes

from a more complex pattern of excitation that mainly involves the HOMO→LUMO+1 excitation but with noticeable contributions of the HOMO-1 to both LUMO and LUMO+2. A large number of other excitations with lower probabilities ($0.13 < f < 0.27$) add up to a quite broad band that, according to the calculations, extends between 450 and 700 nm.

The second, high energy, band is seen in Figure S8 extending between 300 and ca. 420 nm. It is also formed by several high and low-probability transitions. The most intense ones peak at 407 nm ($f = 0.70$), 401 nm ($f = 0.42$), 348 nm ($f = 0.68$) and 340 nm ($f = 0.55$). Excited states at higher energies (wavelength below 300 nm) have not been calculated.

To have an idea of what electronic rearrangements are taking place upon excitation to S_1 we have analyzed the Mulliken atomic charges of the central phenyl ring and the three acetylene groups that bond to the corresponding BODIPY units. There is a noticeable charge transfer from the BODIPYs to the central part of the molecule that amounts to 0.1495 a.u. without nuclear relaxation in the S_1 state and to 0.2126 a.u. between the S_0 and S_1 minimum energy geometries.

Finally we have also analyzed the internal rotation of MD2 in order to find additional conformers in the ground electronic state. In that case there are three BODIPY fragments that can rotate but just one additional rotamer different from the original one that is obtained by rotation of just one BODIPY unit. As in the case of MD2, a reaction coordinate calculation of the internal rotation of a BODIPY unit has been performed and the obtained results show that the energy barrier for this internal rotation is very small (1.21 kcal/mol) so that again free rotation is to be expected (at least in gas phase). Now the rotamer obtained after 180 degrees rotation is not equivalent to the original one (as one of the three BODIPY units points towards the reverse side) but the difference in

energy between both rotamers is negligible (0.12 kcal/mol). We have also calculated the absorption and emission electronic spectra of this additional equilibrium structure. Even if now the ground electronic state geometry is no longer D_{3h} and so there is no degeneracy of the excited electronic states, the obtained results are almost identical to the ones of the initial structure with differences between equivalent bands that never exceed 2 nm. The only remarkable difference is that whereas otherwise degenerate bands appear almost at the same wavelength (they differ by less than 2nm), the oscillator strengths may be now quite disparate. However this difference has no repercussion on the predicted shape of the electronic spectra that is virtually identical to the one depicted in Figure S8.

	6-31G(d,p)			**6-31+G(d,p)**			
	E(eV)	λ(nm)	f	E(eV)	λ(nm)	f	Excitation
S_1(opt.)	2.08	625	1.02	2.15	607	0.65	H→L
S_1(FC)	2.17	571	1.14	2.26	548	0.78	H→L
S_2	2.69	461	0.05	2.68	462	0.03	H-1→L
S_3	3.06	405	0.65	3.14	394	0.75	H-2→L
S_4	3.85	322	0.93	3.83	324	0.55	H→L+1
S_5	3.90	318	0.00	3.87	320	0.00	H-3→L

Table S1. Excitation energies of MD1 for different methods

Solvent	Absorption	Emission	Shift
	λ_{abs} (nm)	λ_{em} (nm)	$\lambda_{abs} - \lambda_{em}$ (cm^{-1})
DCM	562	595	1020
ACN	557	593	1090
MeOH	555	593	1155
TAC	557	593	1090

Table S2. Values of the maximum intensity wavelengths observed in the absorbance and spectral shift of the emission maximum (λ_{pump} = 490 nm) for MD1 in various solvents.

Solvent	Dipol moment (D, 20 °C)	f(ε,n)	Viscosity (cP, 25°C)
DCM	1.14	0.472	0.41
ACN	3.44	0.711	0.34
MeOH	2.87	0.711	0.54
TAC	2.73	0.324	17.4

Table S3. Values of the dipole moments, polarity functions and viscosities of the solvents used in the experiments

Solvent	Quantum yield (%)		
	MD2	MD1	CMPBDP
DCM	17 ± 4.3	36 ± 7.2	1.8 ± 0.72
ACN	7 ± 2.1	25 ± 5	1.3 ± 0.68
MeOH	11 ± 3	30 ± 9	1.5 ± 0.67
TAC	37 ± 7.4	38 ± 7.4	-

Table S4. Values of the quantum yield of MD1, MD2 and CMPBDP in different solvents.

Solvent	Absorption		Emission		Shift	
	λ_{abs1} (nm)	λ_{abs2} (nm)	λ_{em1} (nm)	λ_{em2} (nm)	$\lambda_{abs1} - \lambda_{em1}$ (cm^{-1})	$\lambda_{abs2} - \lambda_{em2}$ (cm^{-1})
DCM	520	555	530	575	330	690
ACN	515	545	525	570	300	840
MeOH	515	540	525	565	295	820
TAC	520	550	525	570	295	700

Table S5. Values of the maximum intensity wavelengths observed in the absorbance and spectral shift of the emission maximum (λ_{pump} = 490 nm) for MD2 in various solvents.

Solvent	Absorption λ_{abs2} (nm)	Emission λ_{em} (nm)
DCM	540	515
ACN	515	520
MeOH	525	520

Table S6. Values of the maximum intensity wavelengths observed in the absorbance and spectral shift of the emission maximum (λ_{pump} = 490 nm) for CMPBDP in various solvents.

MD1 in DCM					
λ_{pump} = 371 nm					
λ_{obs} (nm)	A_1/C_1 (%)	τ_1 (ns)	A_2/C_2(%)	τ_2 (ns)	χ^2
545	6/1	0.52	94/99	3.7	1.09
560	5/1	0.52	95/99	3.7	1.06
580	5/1	0.52	95/99	3.7	1.04
600	4/1	0.52	96/99	3.7	1.04
640	5/1	0.52	95/99	3.7	1.01
670	2/1	0.52	98/99	3.7	1.43
λ_{pump} = 470 nm					
545	7/1	0.57	93/99	3.7	1.14
560	5/1	0.57	95/99	3.7	1.02
580	5/1	0.57	95/99	3.7	1.03
600	5/1	0.57	95/99	3.7	1.10
640	5/1	0.57	95/99	3.7	1.03
670	5/1	0.57	95/99	3.7	1.03

Table S7. Values of fluorescence lifetimes (τi) and normalized (to 100) pre-exponential factors (Ai) obtained from a global multiexponential fits of the emission decays of MD1 in DCM solution upon excitation at 371 and 470 nm.

MD1 in ACN					
λ_{pump} = 371 nm					
λ_{obs} (nm)	A_1/C_1 (%)	τ_1 (ns)	A_2/C_2(%)	τ_2 (ns)	χ^2
545	13/2	0.52	87/98	3.4	1.05
560	13/2	0.52	87/98	3.4	1.14
580	8/1	0.52	92/99	3.4	1.08
600	8/1	0.52	92/99	3.4	1.09
640	9/1	0.52	92/99	3.4	1.09
670	9/1	0.52	91/99	3.4	1.06
λ_{pump} = 470 nm					
545	12/2	0.51	88/98	3.4	1.11
560	11/1	0.51	89/99	3.4	1.05
580	9/1	0.51	95/99	3.4	1.11
600	10/1	0.51	90/99	3.4	1.09
640	11/2	0.51	90/98	3.4	1.11

Table S8. Values of fluorescence lifetimes (τi) and normalized (to 100) pre-exponential factors (Ai) obtained from a global multiexponential fits of the emission decays of MD1 in ACN solution upon excitation at 371 and 470 nm.

MD1 in MeOH					
λ_{pump} = 371 nm					
λ_{obs} (nm)	A_1/C_1 (%)	τ_1 (ns)	A_2/C_2 (%)	τ_2 (ns)	χ^2
545	7/1	0.57	93/99	3.2	1.14
560	5/1	0.57	95/99	3.2	1.02
580	5/1	0.57	95/99	3.2	1.03
600	5/1	0.57	95/99	3.2	1.10
640	5/1	0.57	95/99	3.2	1.03
670	5/1	0.57	95/99	3.2	1.03
λ_{pump}= 470 nm					
545	2/2	0.52	98/98	3.2	1.16
560	2/2	0.52	98/98	3.2	1.05
580	5/1	0.52	95/99	3.2	1.10
600	5/1	0.52	95/99	3.2	1.06
640	6/1	0.52	94/99	3.2	1.07
670	5/2	0.52	95/98	3.2	1.15

Table S9. Values of fluorescence lifetimes (τi) and normalized (to 100) pre-exponential factors (Ai) obtained from a global multiexponential fits of the emission decays of MD1 in MeOH solution upon excitation at 371 and 470 nm.

MD1 in TAC							
λ_{pump} = 371 nm							
λ_{obs}(nm)	A_1/C_1 (%)	τ_1 (ns)	A_2/C_2(%)	τ_2 (ns)	A_3/C_3(%)	τ_3 (ns)	χ^2
545	57/4	0.11	6/5	1.1	37/91	3.8	1.18
560	44/2	0.11	5/2	1.1	51/96	3.7	1.06
580	19/1	0.16	4/2	1.1	77/97	3.7	1.04
600	-	0.19	5/1	1.2	95/99	3.9	1.09
640	-	-	5/1	1.1	95/99	3.5	1.08
670	-	-	5/2	1.1	95/98	3.5	1.05
MD1 in TAC							
λ_{pump} = 470 nm							
545	47/4	0.12	19/22	1.2	34/74	3.8	1.03
560	47/3	0.12	19/22	1.3	33/75	3.8	1.12
580	30/2	0.14	19/15	1.5	51/83	3.5	1.14
600	-	-	5/3	1.1	92/97	4.0	1.09
640	-	-	6/3	1.1	94/97	3.9	1.14
670	-	-	5/3	1.1	95/97	3.9	1.19

Table S10. Values of fluorescence lifetimes (τi) and normalized (to 100) pre-exponential factors (Ai) obtained from a global multiexponential fits of the emission decays of MD1 in TAC solvent upon excitation at 371 nm.

MD2 in DCM							
λ_{pump} = 371 nm							
λ_{obs} (nm)	A_1/C_1 (%)	τ_1 (ns)	A_2/C_2 (%)	τ_2 (ns)	A_3/C_3 (%)	τ_3 (ns)	χ^2
525	10/1	0.11	16/5	1.0	74/94	4.8	1.11
550	13/1	0.11	10/3	0.9	74/96	3.7	1.06
560	14/1	0.11	5/2	1.0	81/97	3.6	1.06
580	11/1	0.11	5/1	1.2	84/98	3.6	1.02
590	13/1	0.21	5/2	1.1	82/97	3.6	1.07
620	14/1	0.12	5/2	1.1	81/97	3.6	1.03
λ_{pump} = 470 nm							
525	38/2	0.10	13/6	1.1	49/92	4.5	1.15
550	35/1	0.10	11/5	1.1	54/94	3.8	1.02
560	13/1	0.13	8/3	1.1	79/96	3.7	1.01
575	9/1	0.12	6/2	0.9	85/97	3.6	1.06
600	10/1	0.13	6/2	0.8	84/97	3.8	1.09
620	13/1	0.13	5/2	0.9	82/97	3.6	1.10

Table S11. Values of fluorescence lifetimes (τi) and normalized (to 100) pre-exponential factors (Ai) obtained from a global multiexponential fits of the emission decays of MD2 in DCM solution upon excitation at 371 and 470 nm.

MD2 in ACN							
λ_{pump} = 371 nm							
λ_{obs} (nm)	A_1/C_1 (%)	τ_1 (ns)	A_2/C_2 (%)	τ_2 (ns)	A_3/C_3 (%)	τ_3 (ns)	χ^2
525	8/1	0.12	22/4	0.8	70/95	5.5	1.04
550	11/1	0.12	66/32	0.8	23/67	4.4	1.06
560	12/1	0.12	82/70	0.8	6/29	4.2	1.05
575	8/1	0.12	89/89	0.8	3/10	2.7	1.18
600	9/1	0.12	88/89	0.8	3/10	2.6	1.01
620	8/1	0.12	88/88	0.8	4/11	2.4	1.02
λ_{pump} = 470 nm							
525	13/1	0.12	33/9	0.8	54/90	4.8	1.07
550	22/2	0.12	54/36	1.0	24/62	4.0	1.02
560	22/2	0.12	62/50	1.0	16/48	3.6	1.06
575	22/2	0.12	64/55	1.0	14/43	3.4	1.03
600	24/3	0.14	62/53	0.9	14/44	3.3	1.09
620	23/3	0.12	60/50	0.9	17/47	3.3	1.03

Table S12. Values of fluorescence lifetimes (τi) and normalized (to 100) pre-exponential factors (Ai) obtained from a global multiexponential fits of the emission decays of MD2 in ACN solution upon excitation at 371 and 470 nm.

MD2 in MeOH,							
λ_{pump} = 371 nm							
λ_{obs} (nm)	A_1/C_1 (%)	τ_1 (ns)	A_2/C_2 (%)	τ_2 (ns)	A_3/C_3 (%)	τ_3 (ns)	χ^2
515	12/1	0.10	10/2	0.8	78/97	5.4	1.08
525	11/1	0.12	15/3	0.8	74/96	5.5	1.07
545	7/1	0.14	2/1	0.8	91/98	3.2	1.02
560	7/1	0.17	-	-	93/99	3.2	1.08
620	8/1	0.17	-	-	92/99	3.2	1.10
λ_{pump} = 470 nm							
525	8/1	0.11	10/2	0.8	82/97	5.4	1.06
550	32/2	0.10	29/13	1.0	39/85	4.7	1.04
560	29/2	0.13	37/23	1.0	34/75	4.2	1.09
575	30/2	0.10	38/26	1.1	32/72	4.2	1.16
600	31/2	0.11	39/27	1.1	30/71	3.5	1.13
620	30/2	0.12	40/31	1.1	30/67	3.5	1.03

Table S13. Values of fluorescence lifetimes (τi) and normalized (to 100) pre-exponential factors (Ai) obtained from a global multiexponential fits of the emission decays of MD2 in MeOH solution upon excitation at 371 and 470 nm.

MD2 in TAC							
λ_{pump} = 371 nm							
λ_{obs} (nm)	A_1/C_1 (%)	τ_1 (ns)	A_2/C_2 (%)	τ_2 (ns)	A_3/C_3 (%)	τ_3 (ns)	χ^2
525	37/2	0.15	15/5	1.3	48/93	4.9	1.08
550	27/2	0.16	14/5	1.3	59/93	3.6	1.02
560	16/1	0.18	9/3	1.3	75/96	3.5	1.07
575	-	-	5/2	1.3	95/98	3.5	1.08
600	-	-	5/2	1.3	95/98	3.5	1.08
620	-	-	5/2	1.3	95/98	3.5	1.06
λ_{pump} = 470 nm							
525	16/1	0.15	14/5	1.3	70/94	5.0	1.08
550	28/2	0.20	17/8	1.3	54/90	4.5	1.22
560	19/1	0.14	9/4	1.3	72/95	3.8	1.04
575	-	-	6/2	1.3	94/98	3.7	1.08
600	-	-	7/2	1.3	93/98	3.7	1.06
620	-	-	7/2	1.3	93/98	3.7	1.10

Table S14. Values of fluorescence lifetimes (τi) and normalized (to 100) pre-exponential factors (Ai) obtained from a global multiexponential fits of the emission decays of MD2 in TAC solution upon excitation at 371 nm.

CMPBDP in DCM							
λ_{pump} = 371 nm							
λ_{obs} (nm)	A_1/C_1 (%)	τ_1 (ns)	A_2/C_2 (%)	τ_2 (ns)	A_3/C_3 (%)	τ_3(ns)	χ^2
500	38/5	0.22	29/12	0.7	33/83	4.3	1.05
530	40/5	0.22	22/8	0.7	39/87	4.2	1.05
560	24/5	0.22	60/44	0.7	16/51	3.1	1.13
590	16/3	0.22	56/35	0.7	28/62	2.8	1.05
600	17/3	0.22	54/33	0.7	29/64	2.8	1.04
650	20/4	0.22	53/34	0.7	27/61	2.8	1.04

Table S15. Values of fluorescence lifetimes (τi) and normalized (to 100) pre-exponential factors (Ai) obtained from a global multiexpon0.80.8ential fits of the emission decays of CMPBDP in DCM suspension upon excitation at 371.

CMPBDP in ACN							
λ_{pump} = 371 nm							
λ_{obs}(nm)	A_1/C_1 (%)	τ_1 (ns)	A_2/C_2 (%)	τ_2 (ns)	A_3/C_3 (%)	τ_3 (ns)	χ^2
500	68/6	0.08	18/17	0.6	13/77	3.9	1.09
525	58/4	0.09	25/15	0.5	17/81	4.0	1.11
560	58/4	0.08	26/16	0.5	16/80	3.5	1.01
600	64/5	0.09	25/25	0.5	11/70	3.4	1.10
620	66/6	0.08	25/27	0.5	9/67	3.4	1.03

Table S16. Values of fluorescence lifetimes (τi) and normalized (to 100) pre-exponential factors (Ai) obtained from a global multiexponential fits of the emission decays of CMPBDP in ACN suspension upon excitation at 371 nm.

CMPBDP in MeOH							
λ_{pump}= 371 nm							
λ_{obs}(nm)	A_1/C_1 (%)	τ_1 (ns)	A_2/C_2 (%)	τ_2 (ns)	A_3/C_3 (%)	τ_3 (ns)	χ^2
500	50/4	0.11	22/12	0.8	28/84	4.2	1.09
530	50/4	0.11	27/14	0.6	23/82	4.3	1.11
560	34/4	0.11	48/27	0.6	18/69	3.8	1.01
590	36/4	0.11	48/32	0.6	16/64	3.4	1.10
620	76/11	0.11	19/31	0.5	5/58	3.3	1.03
650	80/15	0.11	16/31	0.5	4/54	3.2	1.10

Table S17. Values of fluorescence lifetimes (τi) and normalized (to 100) pre-exponential factors (Ai) obtained from a global multiexponential fits of the emission decays of CMPBDP in MeOH suspension upon excitation at 371.

MD1 in DCM					
λ_{em} (nm)	τ_1 (ps)	A_1 (%)	τ_2 (%)	A_2 (%)	Offset (%)
545	0.4	51	2	31	18
560	0.4	45	2	30	25
575	0.3	18	2	29	53
600	0.4	(-) 8	3	(-) 2	90
630	0.3	(-) 11	2	(-) 10	79
670	0.4	(-) 11	2	(-) 14	75

Table S18. Values of time constants (τi) and normalized (to 100) pre-exponential factors (Ai) of the multiexponential functions used to fit the fs-emission signals of MD1 in DCM upon excitation at 505 nm.

MD1 in ACN					
λ_{em} (nm)	τ_1 (ps)	A_1 (%)	τ_2 (%)	A_2 (%)	Offset (%)
545	0.3	70	2	18	12
560	0.3	44	2	26	30
575	0.4	20	2	17	63
600	0.4	(-) 10	2	(-) 4	86
630	0.4	(-) 16	2	(-) 6	78
670	0.4	(-) 23	3	(-) 4	76

Table S19. Values of time constants (τi) and normalized (to 100) pre-exponential factors (Ai) of the multiexponential functions used to fit the fs-emission signals of MD1 in ACN upon excitation at 505 nm.

MD1 in MeOH					
λ_{em} (nm)	τ_1 (ps)	A_1 (%)	τ_2 (%)	A_2 (%)	Offset (%)
545	0.4	38	7	23	39
560	0.4	24	7	21	55
575	0.4	15	7	20	65
600	0.4	(-) 16	-	-	84
630	0.4	(-) 15	5	(-) 2	83
670	0.4	(-) 17	6	(-) 2	81

Table S20. Values of time constants (τi) and normalized (to 100) pre-exponential factors (Ai) of the multiexponential functions used to fit the fs-emission signals of MD1 in MeOH upon excitation at 505 nm.

MD1 in TAC					
λ_{em} (nm)	τ_1 (ps)	A_1 (%)	τ_2 (%)	A_2 (%)	Offset (%)
545	0.4	42	7	24	34
560	0.4	27	7	21	52
575	-	-	5	10	90
600	0.4	(-) 10	6	(-) 6	84
630	0.4	(-) 10	6	(-) 3	84
670	0.4	(-) 9	7	(-) 11	80

Table S21. Values of time constants (τi) and normalized (to 100) pre-exponential factors (Ai) of the multiexponential functions used to fit the fs-emission signals of MD1 in TAC upon excitation at 505 nm.

MD2 in DCM							
λ_{em} (nm)	τ_1 (ps)	A_1 (%)	τ_2 (%)	A_2 (%)	τ_3 (%)	A_3 (%)	Offset (%)
530	0.3	68	4	15	-	-	17
545	0.3	53	3	20	-	-	27
560	0.4	28	4	16	-	-	56
575	-	-	3	9	-	-	91
600	0.4	(-) 6	3	(-) 1	-	-	96
650	-	-	3	(-) 38	3	37	25

Table S22. Values of time constants (τi) and normalized (to 100) pre-exponential factors (Ai) of the multiexponential functions used to fit the fs-emission signals of MD2 in DCM upon excitation at 505 nm.

MD2 in ACN					
λ_{em} (nm)	τ_1 (ps)	A_1 (%)	τ_2 (%)	A_2 (%)	Offset (%)
530	0.3	65	4	13	22
545	0.3	56	5	14	30
560	0.3	10	5	30	60
575	0.3	13	-	-	87
600	-	-	4	6	94
650	0.3	(-) 12	-	-	88

Table S23. Values of time constants (τi) and normalized (to 100) pre-exponential factors (Ai) of the multiexponential functions used to fit the fs-emission signals of MD2 in ACN upon excitation at 505 nm.

MD2 in MeOH					
λ_{em} (nm)	τ_1 (ps)	A_1 (%)	τ_2 (%)	A_2 (%)	Offset (%)
530	0.3	18	13	20	62
545	0.3	13	11	22	71
560	0.3	12	13	20	74
575	-	-	7	14	86
600	-	-	7	13	87
650	0.3	(-) 9	7	10	81

Table S24. Values of time constants (τi) and normalized (to 100) pre-exponential factors (Ai) of the multiexponential functions used to fit the fs-emission signals of MD2 in MeOH upon excitation at 505 nm.

MD2 in TAC					
λ_{em} (nm)	τ_1 (ps)	A_1 (%)	τ_2 (%)	A_2 (%)	Offset (%)
530	0.3	48	6	12	40
545	0.3	37	8	16	47
560	0.3	16	6	7	77
575	-	-	-	-	100
600	0.3	17	6	3	80
650	0.3	(-) 12	-	-	88

Table S25. Values of time constants (τi) and normalized (to 100) pre-exponential factors (Ai) of the multiexponential functions used to fit the fs-emission signals of MD2 in TAC upon excitation at 505 nm.

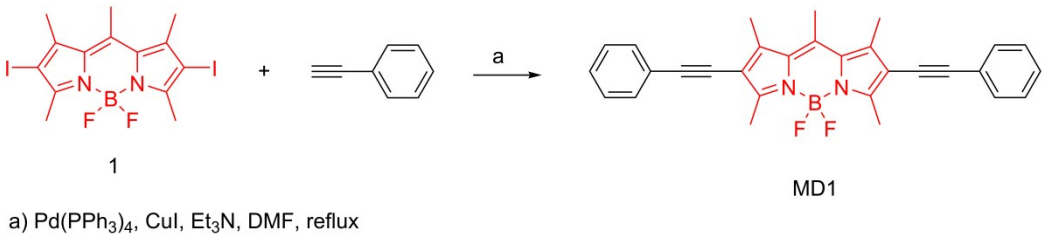

Scheme S1: Synthesis of MD1.

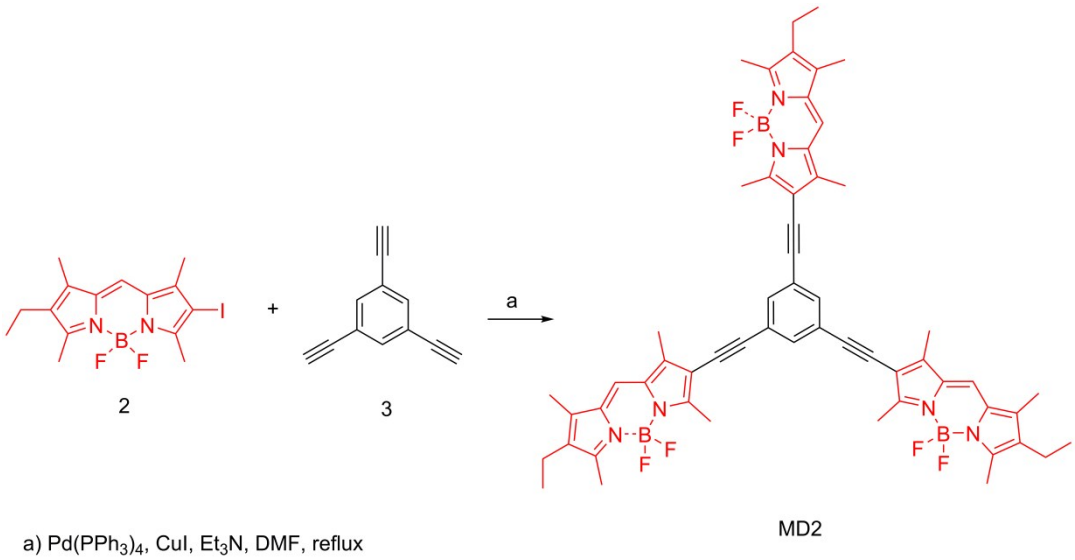

Scheme S2: Synthesis of MD2.

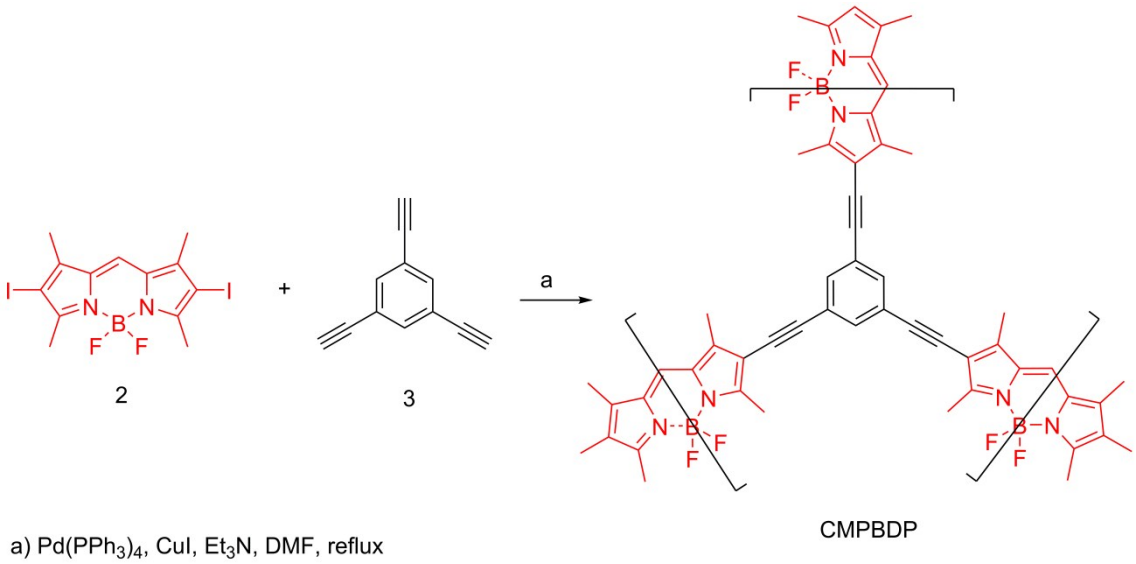

Scheme S3: Synthesis of CMPBDP.

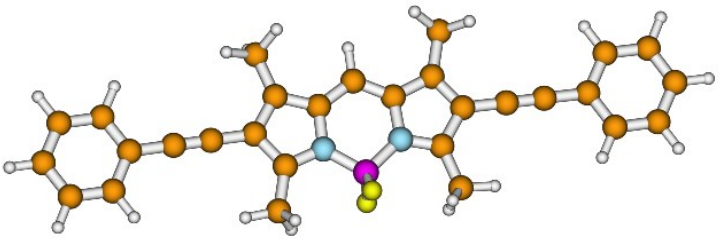

Scheme S4: Equilibrium geometry of MD1 at S_0.

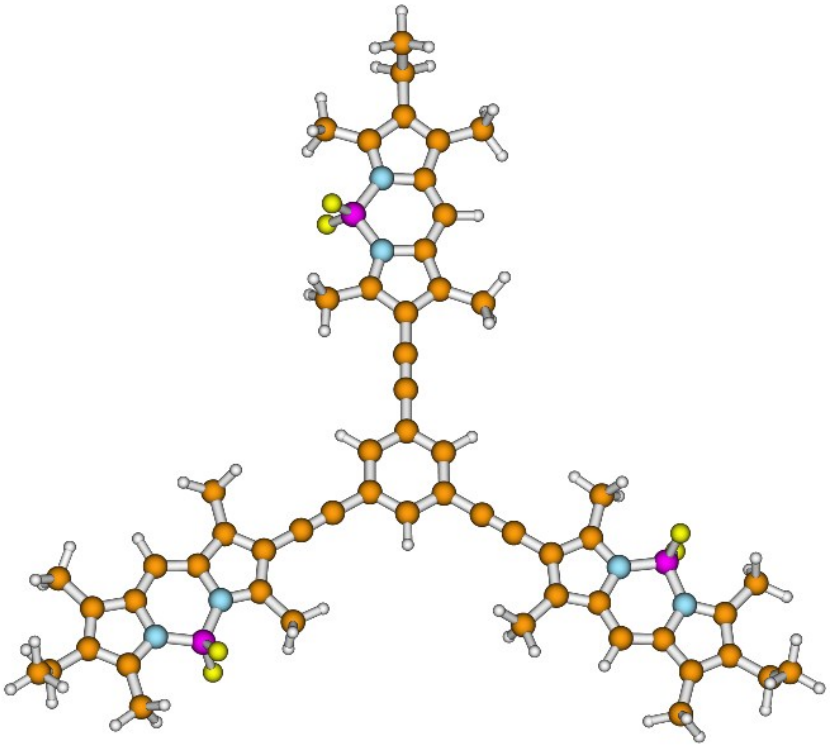

Scheme S5: Equilibrium geometry of MD2 at S_0.

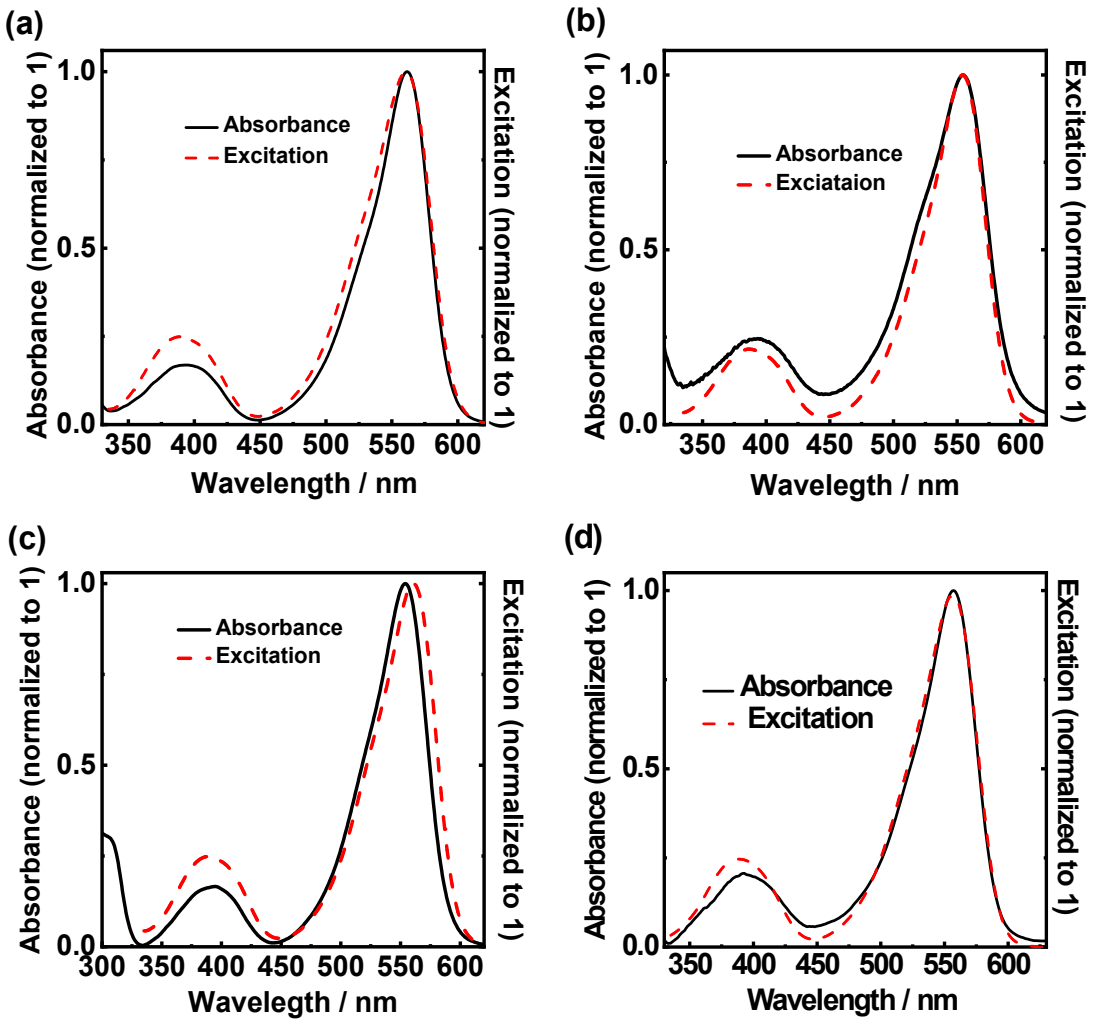

Figure S1. Normalized (to 1) absorption (black solid line) and excitation (red dashed line) spectra of MD1 in (a) DCM, (b) ACN, (c) MeOH, (d) TAC. The excitation spectra were observed at 650 nm.

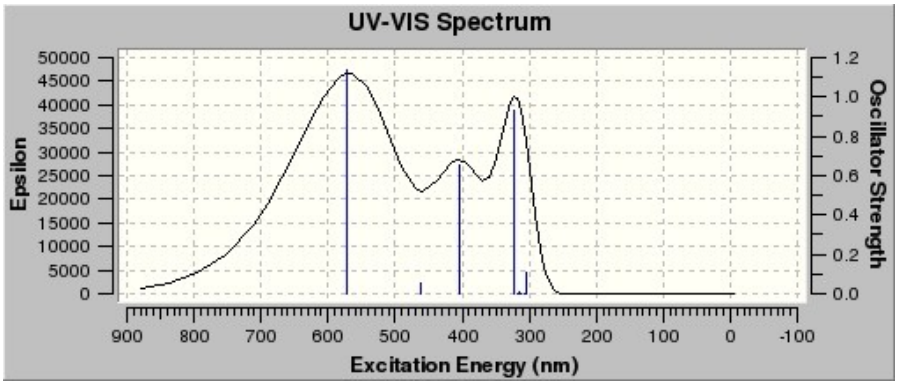

Figure S2: Absorption spectrum of MD1. Vertical blue lines indicate the exact position of the excitation energy and the oscillator strength whereas the bands are drawn assuming a standard Gaussian shape.

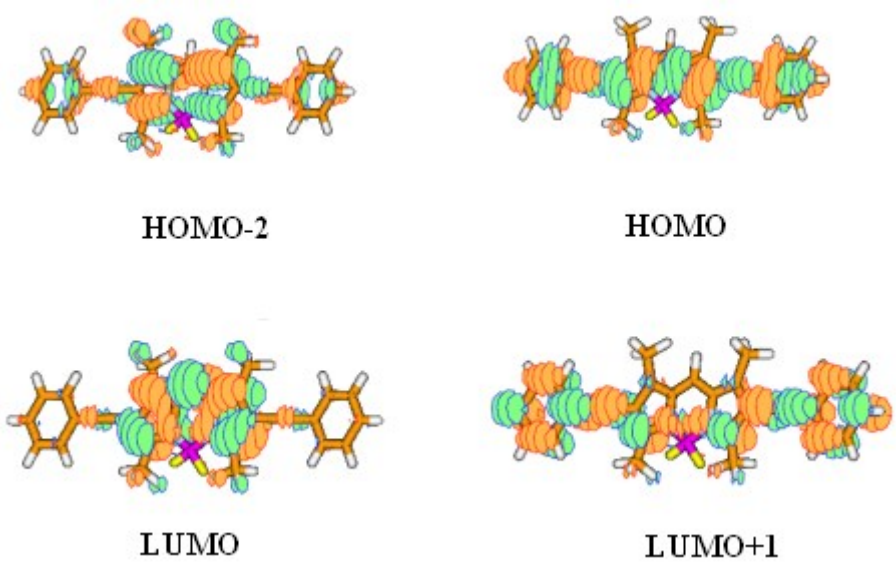

Figure S3: Molecular orbitals of MD1 involved in the allowed electronic transitions.

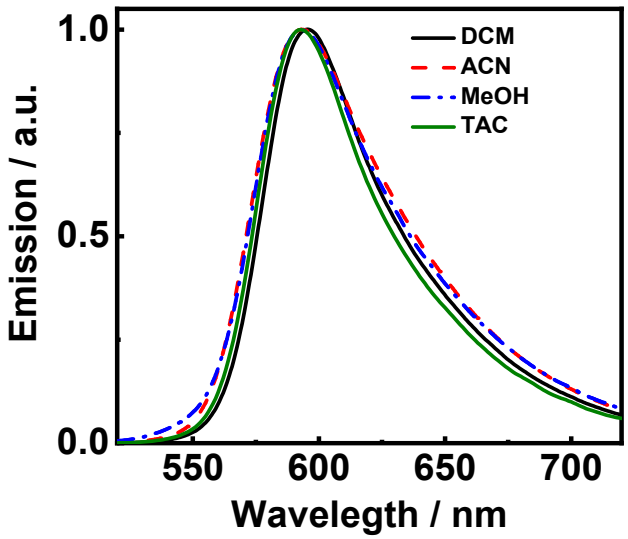

Figure S4. Normalized (to the maximum of intensity) emission spectra of MD1 in DCM (black solid line), ACN (red dashed line), MeOH (blue dashed dotted line), TAC (green solid line) upon excitation at 370 nm.

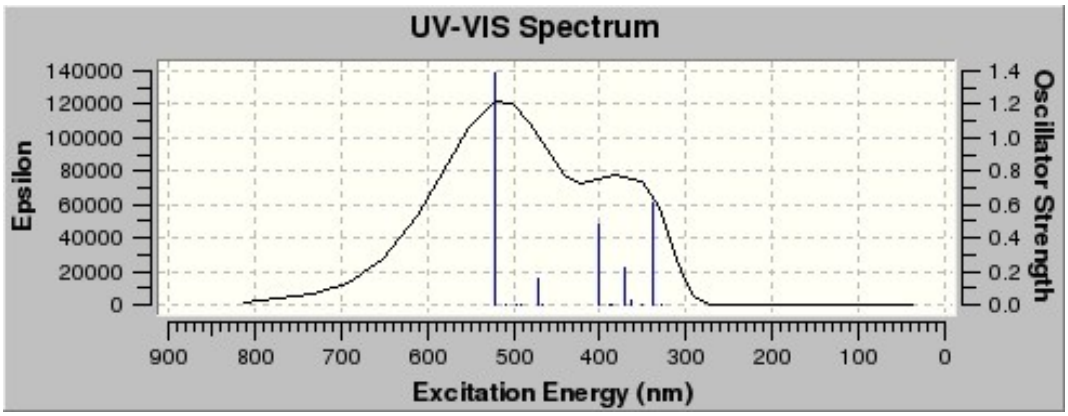

Figure S5: Absorption spectrum of MD2. Vertical blue lines indicate the exact position of the excitation energy and the calculated oscillator strength whereas the bands are shaped assuming a standard Gaussian shape.

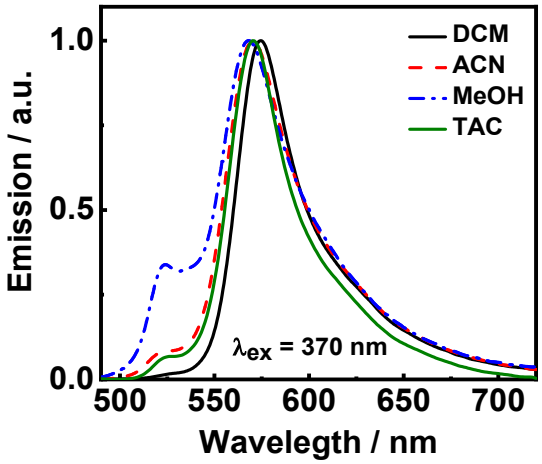

Figure S6. Normalized (to the maximum of intensity) emission spectra of MD2 in DCM (black solid line), MeOH (red dashed line), ACN (blue dashed dotted line), TAC (green solid line) upon excitation at 370 nm.

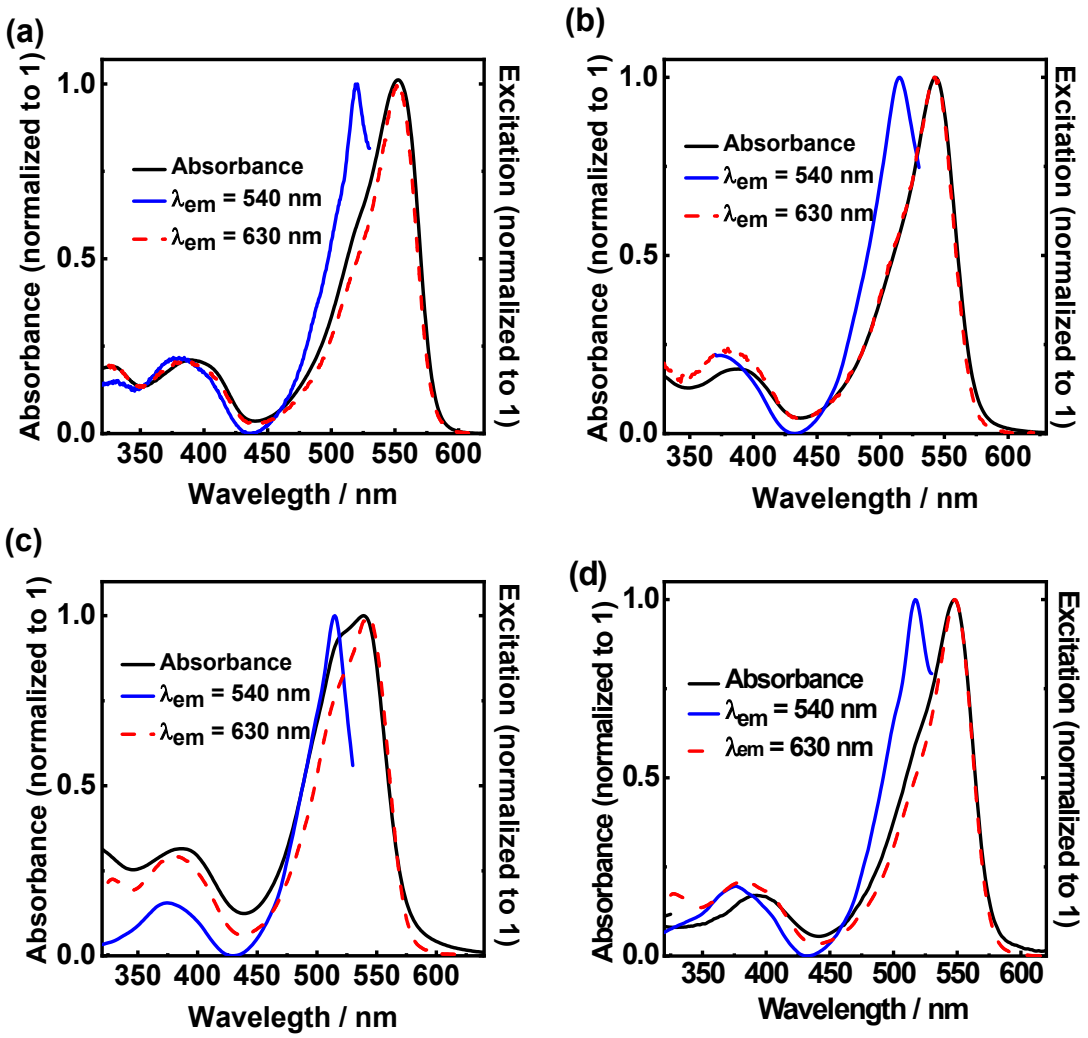

Figure S7. Normalized to 1 absorption (black solid line) and excitation (red dashed line and blue dashed dotted line) spectra of MD2 in (a) DCM, (b) ACN, (c) MeOH and (d) TAC. Observation wavelengths for excitation spectra are indicated in the inset.

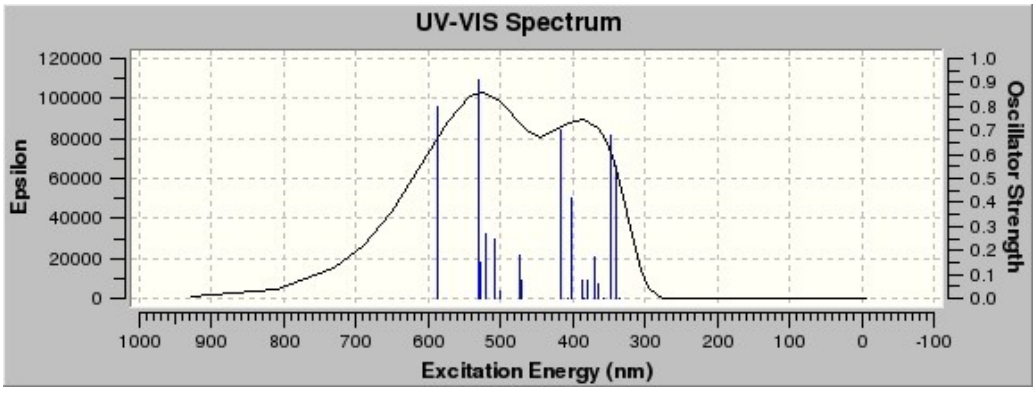

Figure S8: Emission spectrum of MD2. Vertical blue lines indicate the exact position of the excitation energy and the calculated oscillator strength whereas the bands are shaped assuming a standard Gaussian shape.

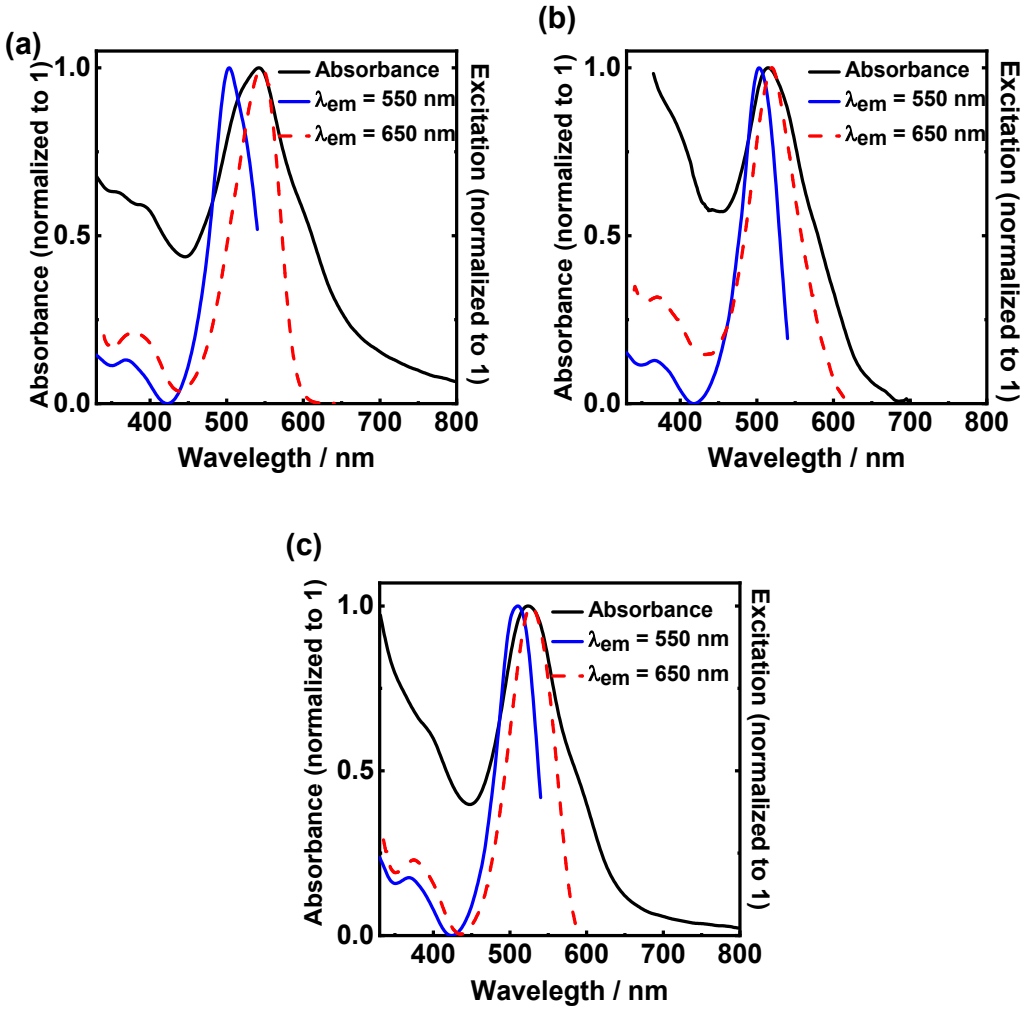

Figure S9. Normalized (to the maximum of intensity) absorption (black solid line) and excitation (red dashed line and blue dashed dotted line) spectra of CMPBDP in (a) DCM, (b) MeOH and (c) ACN. Observation wavelengths for excitation spectra are indicated in the inset.

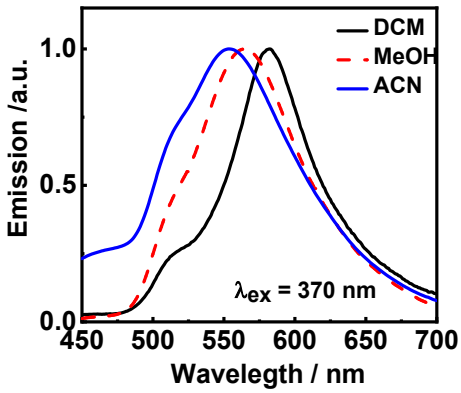

Figure S10. Normalized emission spectra of CMPBDP in DCM (black solid line), ACN (red dashed line), MeOH (blue solid line) excitation at 370 nm.

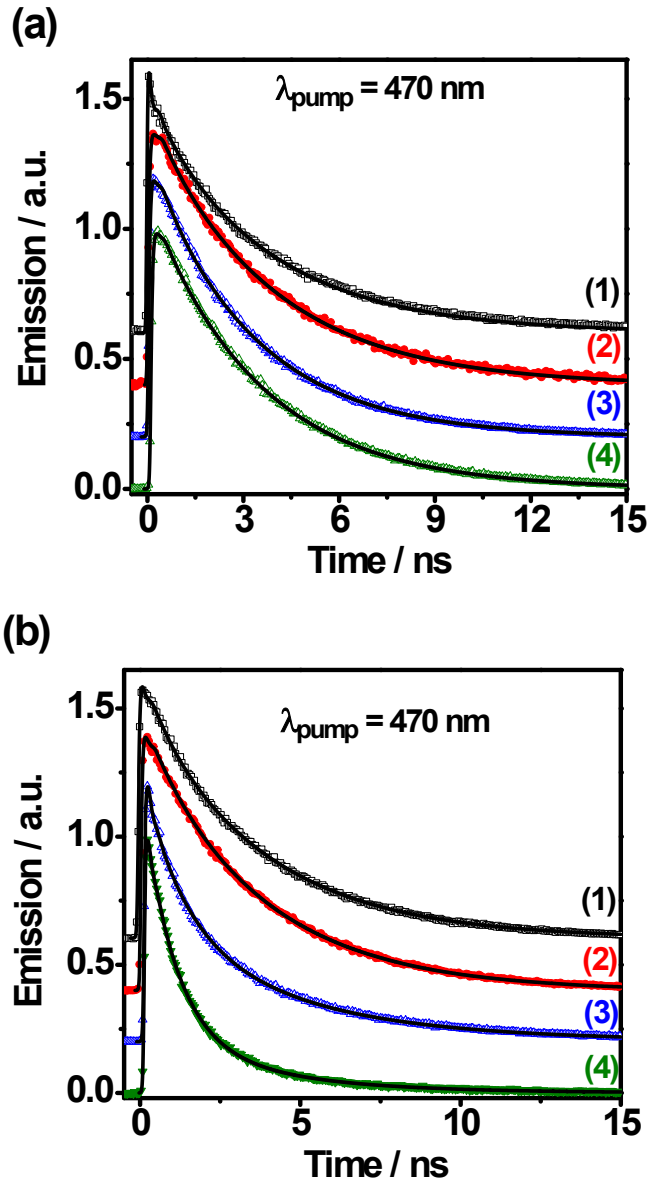

Figure S11. Normalized to 1 magic-angle emission decays of (a) MD1 and (b) MD2 in various solvents (1) TAC, (2) DCM, (3) MeOH, (4) ACN. The excitation and observation wavelengths for all samples were at 470 and 560 nm, respectively. The solid lines are from the best multiexponential fits to the experimental data. For clarity, the TA decay signal was offset on the y axis.

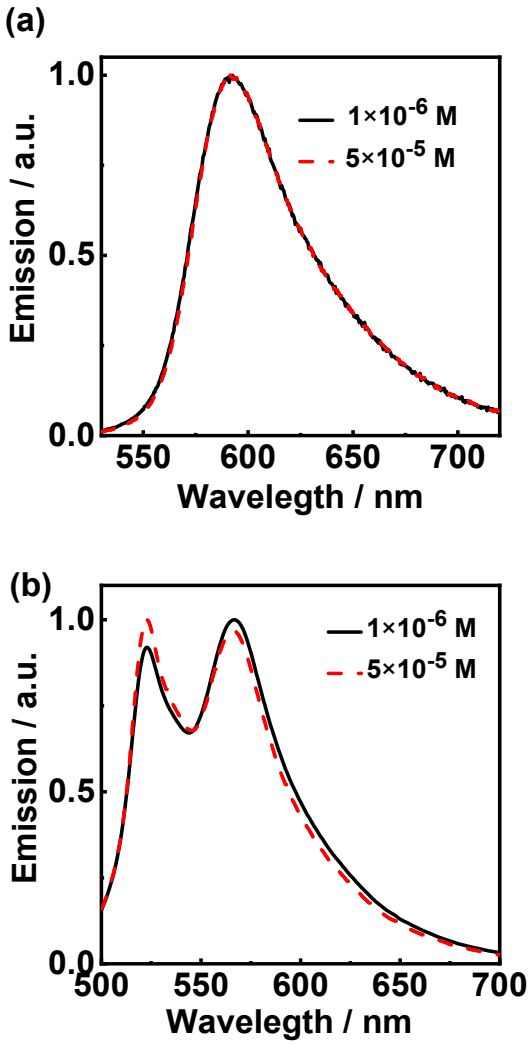

Figure S12. Normalized (to the maximum of intensity) emission spectra of (a) MD1 and (b) MD2 in MeOH at two concentrations (inset). The excitation wavelength for both samples was 470 nm.

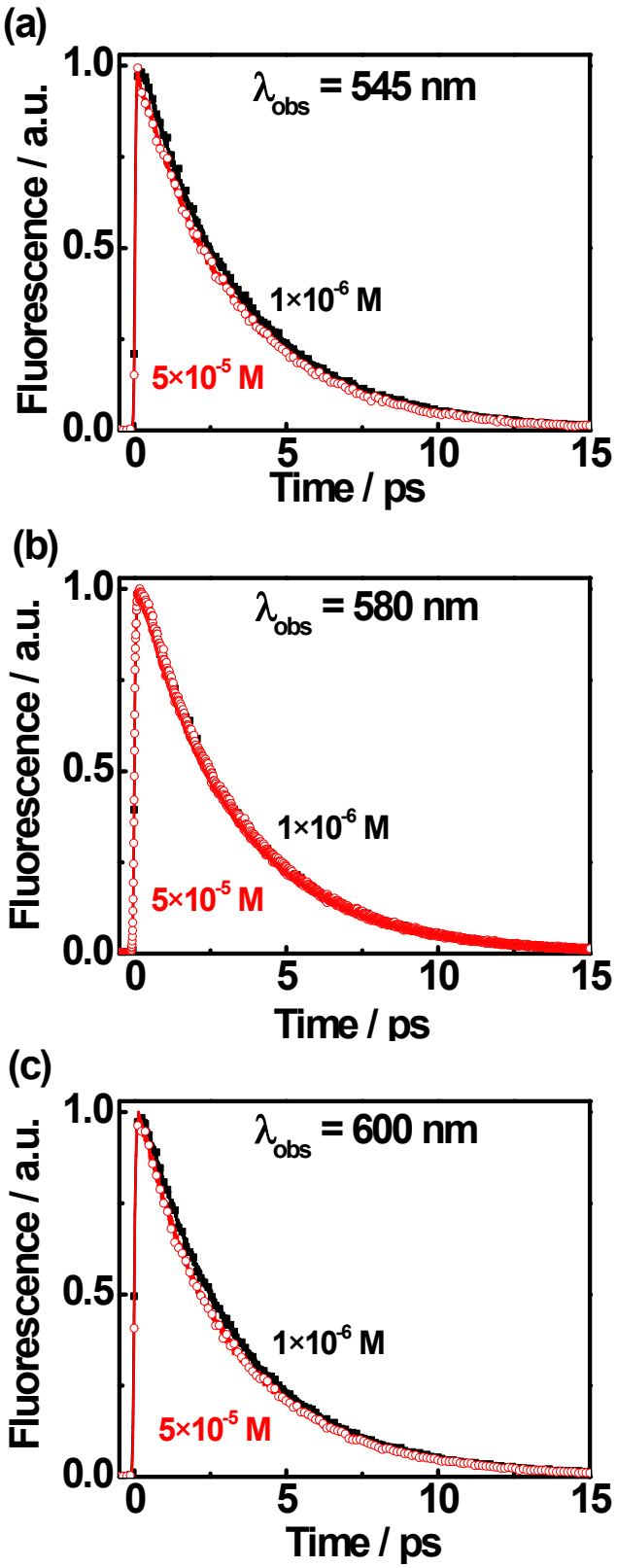

Figure S13. Normalized emission decays of MD1 in MeOH solution, at two concentrations (inset), upon excitation at 470 nm and observing at (a) 545 nm, (b) 560 nm and (c) 600 nm.

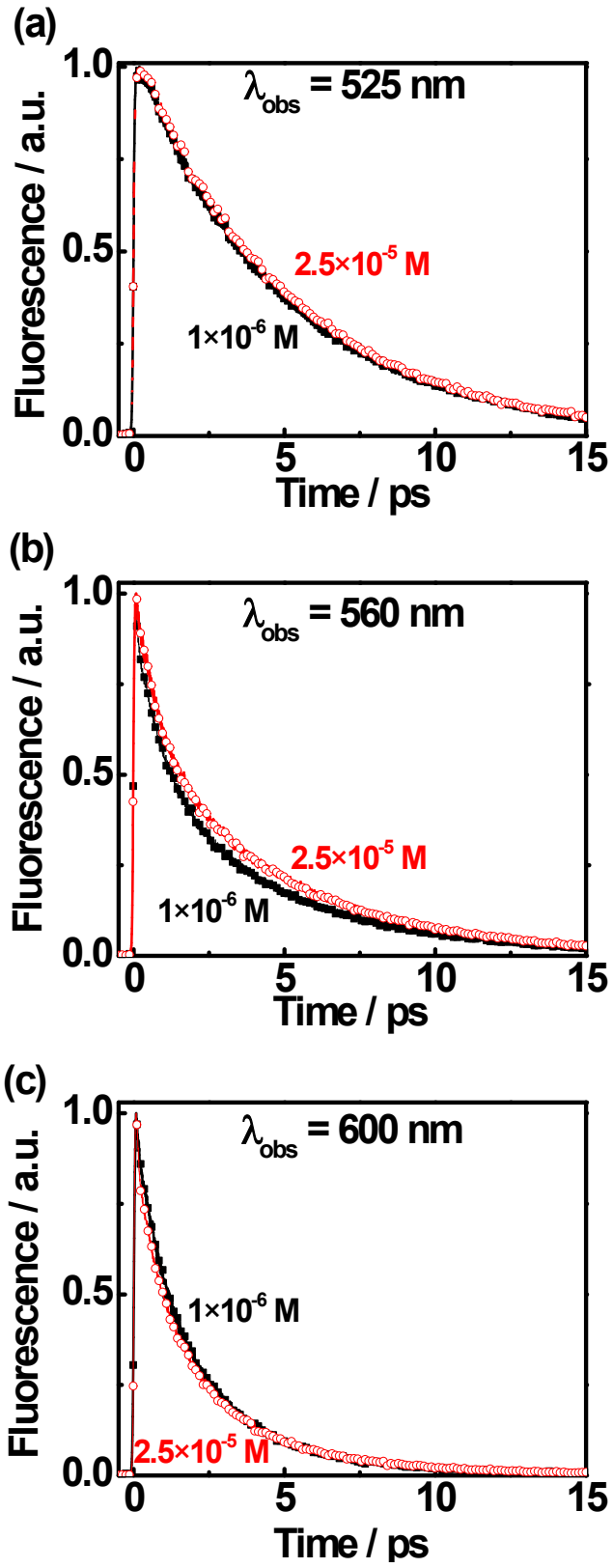

Figure S14. Normalized emission decays of MD2 in MeOH solution, at two concentrations (inset), upon excitation at 470 nm and observing at (a) 545 nm, (b) 560 nm and (c) 600 nm.

Cartesian coordiantes (in Å) in ground state of MD1

1	6	-0.858270	0.006280	1.216641
2	6	-1.531914	0.001201	0.000000
3	6	-0.858270	0.006280	-1.216641
4	6	0.933922	0.011460	2.538901
5	6	-0.220717	0.007200	3.381053
6	6	-1.352355	0.003798	2.545268
7	1	-2.616275	-0.006288	0.000000
8	6	-1.352355	0.003798	-2.545268
9	6	0.933922	0.011460	-2.538901
10	6	-0.220717	0.007200	-3.381053
11	7	0.542988	0.011732	1.253819
12	7	0.542988	0.011732	-1.253819
13	5	1.477104	0.008190	0.000000
14	9	2.278399	1.149830	0.000000
15	9	2.270673	-1.138864	0.000000
16	6	-2.783162	0.022294	-2.975325
17	1	-3.434925	-0.467690	-2.247249
18	1	-3.144365	1.050372	-3.102543
19	1	-2.901032	-0.483022	-3.937577
20	6	-2.783162	0.022294	2.975325
21	1	-3.144365	1.050372	3.102543
22	1	-3.434925	-0.467690	2.247249
23	1	-2.901032	-0.483022	3.937577
24	6	2.364064	0.010600	2.956817
25	1	2.877007	-0.871163	2.560504
26	1	2.880024	0.887654	2.554283
27	1	2.440411	0.014056	4.044694
28	6	2.364064	0.010600	-2.956817
29	1	2.880024	0.887654	-2.554283
30	1	2.877007	-0.871163	-2.560504
31	1	2.440411	0.014056	-4.044694

32	6	-0.201485	0.002125	-4.794026
33	6	-0.201485	0.002125	4.794026
34	6	-0.191417	-0.003906	-6.012416
35	6	-0.191417	-0.003906	6.012416
36	6	-0.179964	-0.009788	-7.437523
37	6	1.040029	-0.010463	-8.145488
38	6	-1.389061	-0.014935	-8.163974
39	6	1.044797	-0.015779	-9.537832
40	1	1.974282	-0.006675	-7.593466
41	6	-1.372789	-0.020526	-9.556217
42	1	-2.331491	-0.014743	-7.626014
43	6	-0.158653	-0.020894	-10.248488
44	1	1.991125	-0.016132	-10.070354
45	1	-2.310918	-0.024598	-10.103056
46	1	-0.150366	-0.025255	-11.334118
47	6	-0.179964	-0.009788	7.437523
48	6	-1.389061	-0.014935	8.163974
49	6	1.040029	-0.010463	8.145488
50	6	-1.372789	-0.020526	9.556217
51	1	-2.331491	-0.014743	7.626014
52	6	1.044797	-0.015779	9.537832
53	1	1.974282	-0.006675	7.593466
54	6	-0.158653	-0.020894	10.248488
55	1	-2.310918	-0.024598	10.103056
56	1	1.991125	-0.016132	10.070354
57	1	-0.150366	-0.025255	11.334118

Cartesian coordiantes (in Å) in first singlet excited state of MD1

1	6	-0.911635	0.017719	1.223074
2	6	-1.605657	0.021306	0.000000
3	6	-0.911635	0.017719	-1.223074

4	6	0.922070	0.016544	2.527243
5	6	-0.224167	0.013357	3.377552
6	6	-1.386262	0.012556	2.540194
7	1	-2.687534	0.026545	0.000000
8	6	-1.386262	0.012556	-2.540194
9	6	0.922070	0.016544	-2.527243
10	6	-0.224167	0.013357	-3.377552
11	7	0.505912	0.018698	1.246941
12	7	0.505912	0.018698	-1.246941
13	5	1.431493	0.017268	0.000000
14	9	2.244521	1.158998	0.000000
15	9	2.241138	-1.126799	0.000000
16	6	-2.811943	0.028116	-2.988614
17	1	-3.453260	-0.544916	-2.311663
18	1	-3.216262	1.048127	-3.033701
19	1	-2.908197	-0.401600	-3.989725
20	6	-2.811943	0.028116	2.988614
21	1	-3.216262	1.048127	3.033701
22	1	-3.453260	-0.544916	2.311663
23	1	-2.908197	-0.401600	3.989725
24	6	2.357554	0.013124	2.922256
25	1	2.866382	-0.868903	2.518577
26	1	2.872351	0.887916	2.510720
27	1	2.452698	0.017379	4.009043
28	6	2.357554	0.013124	-2.922256
29	1	2.872351	0.887916	-2.510720
30	1	2.866382	-0.868903	-2.518577
31	1	2.452698	0.017379	-4.009043
32	6	-0.189000	0.004024	-4.771337
33	6	-0.189000	0.004024	4.771337
34	6	-0.173196	-0.005639	-5.998370
35	6	-0.173196	-0.005639	5.998370

36	6	-0.150762	-0.016362	-7.409682
37	6	1.080079	-0.018241	-8.110593
38	6	-1.359555	-0.025521	-8.147943
39	6	1.093490	-0.028844	-9.499680
40	1	2.008499	-0.011314	-7.549533
41	6	-1.330621	-0.036156	-9.536788
42	1	-2.304601	-0.024251	-7.615312
43	6	-0.107843	-0.037845	-10.218094
44	1	2.041926	-0.030211	-10.027729
45	1	-2.262459	-0.043201	-10.093565
46	1	-0.091176	-0.046169	-11.303410
47	6	-0.150762	-0.016362	7.409682
48	6	-1.359555	-0.025521	8.147943
49	6	1.080079	-0.018241	8.110593
50	6	-1.330621	-0.036156	9.536788
51	1	-2.304601	-0.024251	7.615312
52	6	1.093490	-0.028844	9.499680
53	1	2.008499	-0.011314	7.549533
54	6	-0.107843	-0.037845	10.218094
55	1	-2.262459	-0.043201	10.093565
56	1	2.041926	-0.030211	10.027729
57	1	-0.091176	-0.046169	11.303410

Cartesian coordiantes (in Å) in ground state of MD2

1	6	-7.026246	7.238235	0.119943
2	6	-5.677000	6.931126	0.082814
3	6	-5.217119	5.611617	0.086483
4	6	-9.203873	6.807805	0.202352
5	6	-9.064256	8.225525	0.168081
6	6	-7.697188	8.498636	0.116527
7	1	-4.953795	7.738153	0.045364

8	6	-3.904100	5.092000	0.046970
9	6	-5.433624	3.394091	0.128505
10	6	-4.040642	3.687419	0.074341
11	7	-7.987984	6.224770	0.174718
12	7	-6.126402	4.547898	0.134282
13	5	-7.681294	4.695866	0.195062
14	9	-8.165575	4.121547	1.373943
15	9	-8.263448	4.075231	-0.911835
16	6	-2.623607	5.858839	-0.025018
17	1	-2.141227	5.727258	-1.000851
18	1	-2.776376	6.929073	0.130074
19	1	-1.914652	5.503668	0.730099
20	6	-7.036435	9.840617	0.048022
21	1	-5.990233	9.796873	0.360915
22	1	-7.058397	10.243872	-0.971646
23	1	-7.546403	10.565080	0.690341
24	6	-10.461563	6.004663	0.253811
25	1	-10.621508	5.482194	-0.695756
26	1	-10.392457	5.239150	1.031116
27	1	-11.326695	6.639373	0.449736
28	6	-6.082843	2.052949	0.175512
29	1	-6.680398	1.948029	1.086326
30	1	-6.766238	1.928993	-0.670014
31	1	-5.328367	1.265691	0.147973
32	6	-2.999347	2.732674	0.054394
33	6	-2.094403	1.917323	0.037485
34	6	9.795203	2.429428	-0.071412
35	6	8.844749	1.423495	-0.040400
36	6	7.474613	1.698153	-0.051454
37	6	10.531079	4.524009	-0.146679
38	6	11.681169	3.683341	-0.113333
39	6	11.221766	2.366952	-0.064317

40	1	9.171294	0.390121	-0.004216
41	6	6.359551	0.831335	-0.024403
42	6	5.675041	3.011872	-0.095403
43	6	5.219397	1.663049	-0.052087
44	7	9.411121	3.772915	-0.123226
45	7	7.020889	3.022139	-0.094065
46	5	7.938632	4.286148	-0.146079
47	9	7.696347	5.099280	0.962504
48	9	7.693936	4.999091	-1.323544
49	6	6.367817	-0.662398	0.015271
50	1	5.952372	-1.081254	-0.908720
51	1	7.375076	-1.064930	0.141782
52	1	5.748144	-1.033662	0.838480
53	6	12.042379	1.116197	0.000457
54	1	12.402119	0.927322	1.019106
55	1	11.473092	0.238308	-0.314833
56	1	12.924823	1.189533	-0.642552
57	6	10.478168	6.015416	-0.194025
58	1	9.772587	6.346835	-0.960230
59	1	10.124757	6.417053	0.762097
60	1	11.461708	6.437780	-0.403795
61	6	4.850126	4.253019	-0.138711
62	1	5.077446	4.894720	0.718091
63	1	5.076773	4.831958	-1.039298
64	1	3.788553	4.002602	-0.129702
65	6	3.868122	1.250611	-0.040239
66	6	2.707049	0.882079	-0.030030
67	6	-2.782009	-9.674538	-0.106394
68	6	-3.180550	-8.349361	-0.072498
69	6	-2.259778	-7.298248	-0.077281
70	6	-1.332598	-11.356048	-0.182897
71	6	-2.634559	-11.934309	-0.153525

72	6	-3.546969	-10.880236	-0.103481
73	1	-4.239326	-8.117889	-0.040455
74	6	-2.456370	-5.899693	-0.046314
75	6	-0.224281	-6.391934	-0.110131
76	6	-1.167305	-5.325152	-0.066743
77	7	-1.425683	-10.010805	-0.155572
78	7	-0.885620	-7.564059	-0.116418
79	5	-0.246773	-8.989652	-0.168827
80	9	0.571920	-9.187813	0.944466
81	9	0.500904	-9.129567	-1.341782
82	6	-3.756281	-5.163499	-0.011194
83	1	-3.917088	-4.607034	-0.942023
84	1	-4.605759	-5.835675	0.127291
85	1	-3.767019	-4.430704	0.802576
86	6	-5.040325	-10.969801	-0.041460
87	1	-5.383131	-11.218033	0.970273
88	1	-5.517913	-10.029911	-0.328745
89	1	-5.416570	-11.752124	-0.707953
90	6	-0.013407	-12.053861	-0.228195
91	1	0.627431	-11.606839	-0.992569
92	1	0.508634	-11.948368	0.729205
93	1	-0.137142	-13.116933	-0.439041
94	6	1.262834	-6.294527	-0.145845
95	1	1.701717	-6.814975	0.710894
96	1	1.656459	-6.775360	-1.046689
97	1	1.574181	-5.249243	-0.130594
98	6	-0.851530	-3.948172	-0.047590
99	6	-0.590985	-2.758258	-0.032019
100	6	0.302720	1.384936	0.003208
101	6	1.349662	0.446179	-0.017991
102	6	1.046974	-0.927296	-0.027967
103	6	-0.289574	-1.364869	-0.017665

104	6	-1.327449	-0.416012	0.004249
105	6	-1.038001	0.960176	0.014888
106	1	0.530748	2.444432	0.011178
107	1	1.850609	-1.654291	-0.045082
108	1	-2.359042	-0.748297	0.012333
109	6	-10.191835	9.221093	0.157333
110	1	-11.009812	8.861981	0.792767
111	1	-9.847939	10.157475	0.611147
112	6	-10.739406	9.516702	-1.251568
113	1	-11.130367	8.608868	-1.722091
114	1	-11.550508	10.250664	-1.207052
115	1	-9.954993	9.916528	-1.901925
116	6	-2.944495	-13.406241	-0.146597
117	1	-2.223282	-13.939779	-0.776643
118	1	-3.924868	-13.568787	-0.608718
119	6	-2.942485	-14.029956	1.261658
120	1	-3.180110	-15.097570	1.213821
121	1	-1.963585	-13.922295	1.739600
122	1	-3.682487	-13.545924	1.906864
123	6	13.111546	4.148871	-0.103158
124	1	13.742600	3.379880	-0.563083
125	1	13.216057	5.039418	-0.733838
126	6	13.647951	4.463247	1.305988
127	1	13.596391	3.581288	1.952183
128	1	14.691893	4.789830	1.260130
129	1	13.065496	5.258502	1.782155

Cartesian coordiantes (in Å) in first singlet excited state of MD2

1	6	5.171406	-8.632844	0.159667
2	6	3.925527	-8.033257	0.140994
3	6	3.772348	-6.643240	0.109511
4	6	7.391075	-8.700191	0.180691
5	6	6.936351	-10.051826	0.198295
6	6	5.543291	-10.012575	0.184903
7	1	3.039109	-8.657698	0.146565
8	6	2.609098	-5.845408	0.082824
9	6	4.482757	-4.530865	0.068506
10	6	3.058165	-4.505902	0.056536
11	7	6.337438	-7.860025	0.158214
12	7	4.898006	-5.809805	0.099550
13	5	6.382054	-6.301054	0.127480
14	9	7.018531	-5.812399	1.271491
15	9	7.050764	-5.862639	-1.016401
16	6	1.188032	-6.306563	0.072408
17	1	0.707738	-6.076474	-0.885880
18	1	1.105298	-7.382737	0.238270
19	1	0.608073	-5.797700	0.849474
20	6	4.597094	-11.172818	0.177746
21	1	3.601749	-10.889726	0.528894
22	1	4.484687	-11.588683	-0.830835
23	1	4.960176	-11.981282	0.819483
24	6	8.797971	-8.201515	0.177865
25	1	9.048004	-7.768503	-0.796996
26	1	8.923358	-7.409826	0.921066
27	1	9.500933	-9.008277	0.388676
28	6	5.417531	-3.369933	0.052553
29	1	6.054803	-3.379567	0.942092
30	1	6.081451	-3.425917	-0.815475
31	1	4.859266	-2.433432	0.019703

32	6	2.257963	-3.344540	0.025228
33	6	1.556385	-2.348589	-0.000906
34	6	-10.101711	-0.105204	-0.148161
35	6	-8.970340	0.695955	-0.183159
36	6	-7.665317	0.114589	-0.143868
37	6	-11.275914	-2.011536	-0.052655
38	6	-12.213816	-0.947986	-0.119631
39	6	-11.486884	0.249321	-0.179629
40	1	-9.070483	1.771680	-0.240002
41	6	-6.412046	0.693247	-0.166009
42	6	-6.221914	-1.620122	-0.045022
43	6	-5.465476	-0.414055	-0.102502
44	7	-10.010658	-1.504966	-0.070973
45	7	-7.525471	-1.298078	-0.069233
46	5	-8.706520	-2.319804	-0.016648
47	9	-8.625898	-3.063428	1.171680
48	9	-8.612541	-3.195719	-1.110881
49	6	-6.054493	2.140789	-0.240265
50	1	-5.464441	2.361914	-1.138130
51	1	-6.945072	2.772642	-0.262775
52	1	-5.448011	2.447296	0.620623
53	6	-12.006470	1.651709	-0.250829
54	1	-11.900213	2.180412	0.706216
55	1	-11.468570	2.243722	-1.000683
56	1	-13.067386	1.670299	-0.514060
57	6	-11.528489	-3.479538	0.027981
58	1	-11.027418	-4.006195	-0.792300
59	1	-11.119090	-3.895324	0.956470
60	1	-12.596700	-3.698868	-0.011160
61	6	-5.717835	-3.019979	0.035086
62	1	-6.085876	-3.509635	0.942634
63	1	-6.085333	-3.609385	-0.811135

64	1	-4.626783	-3.032510	0.036853
65	6	-4.087664	-0.326482	-0.095614
66	6	-2.859216	-0.228335	-0.088447
67	6	4.963726	8.730921	-0.080842
68	6	5.035517	7.350020	-0.074382
69	6	3.889651	6.547990	-0.098052
70	6	3.957210	10.710317	-0.118715
71	6	5.360461	10.960991	-0.071402
72	6	5.994802	9.720188	-0.047076
73	1	6.008314	6.872059	-0.044926
74	6	3.747909	5.144457	-0.087352
75	6	1.695608	6.156524	-0.143814
76	6	2.357368	4.894941	-0.115885
77	7	3.726579	9.382438	-0.124466
78	7	2.618416	7.135204	-0.133021
79	5	2.337695	8.672870	-0.163967
80	9	1.579196	9.041214	0.947836
81	9	1.657858	9.004620	-1.339007
82	6	4.834234	4.118960	-0.059880
83	1	4.865689	3.555477	-0.999784
84	1	5.817950	4.567532	0.094045
85	1	4.663476	3.392277	0.741369
86	6	7.465170	9.447566	0.023325
87	1	7.837198	9.535082	1.051238
88	1	7.711051	8.443370	-0.330602
89	1	8.028180	10.162823	-0.583885
90	6	2.844175	11.704542	-0.149139
91	1	2.115206	11.436682	-0.918232
92	1	2.311905	11.712631	0.808453
93	1	3.220495	12.709619	-0.343686
94	6	0.228576	6.418645	-0.178873
95	1	-0.074513	7.014581	0.687412

96	1	-0.035550	6.995501	-1.070517
97	1	-0.324859	5.478758	-0.181215
98	6	1.721264	3.635918	-0.108303
99	6	1.179528	2.544442	-0.099103
100	6	-0.657124	-1.285982	-0.043544
101	6	-1.458675	-0.120712	-0.077767
102	6	-0.845803	1.154299	-0.099094
103	6	0.551106	1.267793	-0.084507
104	6	1.336512	0.095946	-0.052374
105	6	0.740504	-1.183007	-0.032126
106	1	-1.129745	-2.260585	-0.027385
107	1	-1.463016	2.044200	-0.124261
108	1	2.416909	0.179710	-0.042490
109	6	7.812899	-11.273987	0.200979
110	1	8.705869	-11.088497	0.809421
111	1	7.279863	-12.095884	0.692026
112	6	8.245408	-11.725552	-1.206712
113	1	8.818281	-10.943252	-1.714825
114	1	8.872342	-12.621245	-1.150610
115	1	7.375547	-11.958161	-1.829034
116	6	6.008777	12.317351	-0.023638
117	1	5.444967	13.019800	-0.648683
118	1	7.007924	12.253498	-0.469164
119	6	6.128702	12.892786	1.400018
120	1	6.610200	13.875782	1.381322
121	1	5.144037	13.007293	1.864502
122	1	6.724290	12.234978	2.040821
123	6	-13.709955	-1.098325	-0.093756
124	1	-14.166086	-0.298734	-0.689533
125	1	-13.997488	-2.036610	-0.582307
126	6	-14.309044	-1.067092	1.325487
127	1	-14.076667	-0.122800	1.828163

128	1	-15.398405	-1.175535	1.292124
129	1	-13.905638	-1.878310	1.939964